

# NaI (Tl) calorimeter calibration and simulation for Coulomb sum rule experiment in Hall-A at Jefferson Lab\*

YAN Xin-Hu(闫新虎)<sup>1,5;1)</sup> C. Alexandre<sup>2</sup> CHEN Jian-Ping(陈剑平)<sup>2</sup> C. Seonho<sup>4</sup>  
LÜ Hai-Jiang(吕海江)<sup>5</sup> M. Zein-Eddine<sup>3</sup> Oh Yoomin<sup>4</sup> S. Vincent<sup>2</sup>  
YE Yun-Xiu(叶云秀)<sup>1</sup> YAO Huan(姚欢)<sup>3</sup>

<sup>1</sup> Department of Modern Physics, University of Science and Technology of China, Hefei 230026, China

<sup>2</sup> Thomas Jefferson National Accelerator Facility, Newport News, VA 23606, USA

<sup>3</sup> Temple University, Philadelphia, PA 19122, USA

<sup>4</sup> Seoul National University, Seoul 151-747, Korea

<sup>5</sup> Huangshan University, Huangshan 245021, China

**Abstract:** A precision measurement of inclusive electron scattering cross sections is carried out at Jefferson Lab in the quasi-elastic region for  ${}^4\text{He}$ ,  ${}^{12}\text{C}$ ,  ${}^{56}\text{Fe}$  and  ${}^{208}\text{Pb}$  targets. The longitudinal ( $R_L$ ) and transverse ( $R_T$ ) response functions of the nucleon need to be extracted precisely in the momentum transfer range  $0.55 \text{ GeV}/c \leq |q| \leq 1.0 \text{ GeV}/c$ . To achieve the above goal, a NaI (Tl) calorimeter is used to distinguish good electrons from background, including pions and low energy electrons rescattered from the walls of the spectrometer magnets. Due to a large set of kinematics and changes in HV settings, a number of calibrations are performed for the NaI (Tl) detector. Corrections for a few blocks of NaI (Tl) with bad or no signal are applied. The resolution of the NaI (Tl) detector after calibration reached  $\frac{\delta E}{\sqrt{E}} \approx 3\%$  at  $E=1 \text{ GeV}$ . The performance of the NaI (Tl) detector is compared with a simulation. The good calibration and background analysis for the NaI(Tl) detector are very important for the reduction of the systematic error of cross sections and the separation of  $R_L$  and  $R_T$ .

**Key words:** Coulomb sum rule, NaI (Tl), calibration, resolution, GEANT4 simulation

**PACS:** 29.30.Dn, 29.40.Mc **DOI:** 10.1088/1674-1137/35/5/017

## 1 Introduction

The study of nucleon properties in a nuclear medium is an essential objective in nuclear physics. The Coulomb sum rule(CSR) provides one of the cleanest means to study nuclear medium effects on the charge response of nucleons [1]. The Coulomb sum  $S_L(q)$  is given by

$$S_L(q) = \frac{1}{Z} \int_{\omega^+}^{\infty} d\omega \frac{R_L(q, \omega)}{\tilde{G}_E(Q^2)^2}, \quad (1)$$

with  $Z$  being the atomic number of the nucleus,  $Q^2$  the four momentum transfer squared,  $q$  the three momentum transfer and  $\omega$  the energy loss. After factoring out an effective nucleon charge form fac-

tor  $\tilde{G}_E(Q^2)^2$ , which is an appropriate sum of neutron and proton charge form factors and the longitudinal response  $R_L(q, \omega)$  is integrated from  $\omega^+$  to infinity where  $\omega^+$  is selected to exclude the elastic peak, the  $S_L(q)$  should approach 1 as  $q \rightarrow \infty$  for a system of non-relativistic nucleons. In this limit  $S_L(q)$  simply measures the total charge divided by  $Z$ . In the Fermi gas model, the asymptotic limit of  $S_L(q)$  is reached for  $q \geq 2k_F \sim 500 \text{ MeV}/c$  where correlations due to the Pauli Blocking effect vanish. Since the ratio of  $R_L$  to  $R_T$  is small at large  $q$ ,  $R_L$  has a large sensitivity to the uncertainties of the cross sections. To make a precision measurement of  $R_L$ , the uncertainties of cross sections need to be at the 1% level. Therefore,  $R_L$  is much harder to determine with good precision

Received 5 August 2010, Revised 21 September 2010

\* Supported by National Natural Science Foundation of China (10605022,10875053) and US Department of Energy (DE-AC05-84ER-40150) under which Jefferson Science Associates operates the Thomas Jefferson National Accelerator Facility

1) E-mail: yanxinhu@mail.ustc.edu.cn

©2011 Chinese Physical Society and the Institute of High Energy Physics of the Chinese Academy of Sciences and the Institute of Modern Physics of the Chinese Academy of Sciences and IOP Publishing Ltd

than  $R_T$ . To achieve the above goal, a NaI (Tl) calorimeter due to its good resolution is used to distinguish good electrons from background for the reduction of systematic error of cross section.

The Jefferson Lab CSR experiment (E05-110) [2] measured the cross sections of quasi-elastic electron scattering on four different targets ( $^4\text{He}$ ,  $^{12}\text{C}$ ,  $^{56}\text{Fe}$  and  $^{208}\text{Pb}$ ) at four different scattering angles ( $15^\circ$ ,  $60^\circ$ ,  $90^\circ$ ,  $120^\circ$ ) with beam energies from 0.4 GeV to 4.0 GeV. The standard Hall-A detector configuration includes two high resolution spectrometers (HRS) [3]. Each HRS has a  $Q_1Q_2DQ_3$  magnet configuration where  $Q_1$ ,  $Q_2$  and  $Q_3$  are quadrupole magnets and  $D$  is a dipole magnet. For the CSR experiment, both HRSs are configured for electron detection. The NaI (Tl) detector is installed in the left HRS. We will focus on the left HRS. The left HRS detector package consists of two Vertical Drift Chambers (VDCs), a pair of plastic scintillator planes, a gas Cerenkov counter and a NaI (Tl) calorimeter. The VDCs are used to determine the particle trajectory. The scintillators made the trigger. The gas Cerenkov counter and the NaI (Tl) calorimeter formed the particle identification (PID) system.

## 2 NaI (Tl) detector

This NaI (Tl) calorimeter was first used at Los Alamos National Laboratory [4] and Brookhaven National Laboratory. The detector was transferred to Jefferson Lab for this experiment. The NaI (Tl) calorimeter was refurbished and reconfigured into three boxes with each box consisting of 90 ( $10 \times 9$  array) blocks. The length, width and height of each individual block are 30.5 cm, 6.35 cm and 6.35 cm, respectively. Because the total length of 30.5 cm is 11.5 radiation length, an electron with less than 0.55 GeV could deposit most of its energy in the calorimeter. An electron with energy greater than 0.55 GeV would have some energy leaked. Since a few blocks have bad or no signal during the experiment, the missing energy corrections for the bad blocks are studied and corrected in the calibration. The following section will focus on the middle box of the NaI (Tl) detector.

## 3 NaI (Tl) Calibration

An electromagnetic cascade generates a shower of low energy photons and electron-positron pairs when a high energy electron hits the NaI (Tl) calorimeter. As the cascade propagates, a large part of the original particle's energy is converted to light, which usually

covers several blocks. The light in each block is collected in a photomultiplier tube (PMT). The output signal from the PMT is then digitized with an analog-to-digital-converter (ADC). There is a conversion between the raw ADC values and the total energy deposition in the NaI (Tl) calorimeter. To accomplish this conversion, one needs to determine the calibration coefficients for each of the calorimeter blocks. In general, the electromagnetic cascade is spread over several adjacent blocks, and the output signal must be integrated over the entire calorimeter volume to obtain the total detectable energy. If the calorimeter has been calibrated properly, the total deposited energy  $E$  should be proportional to the incident particle's energy (or momentum  $p$ ).

### 3.1 Calibration event selection

To obtain good calibration coefficients, an electron sample needs to be selected. This is accomplished by selecting a run with less background from pions. Runs in the quasi-elastic electron scattering settings are used to do the calibration. The following tight cuts are applied to select electron samples:

- (1) An event reconstruction in the spectrometer detector package is successful.
- (2) Only one track had been reconstructed by the VDC system.
- (3) The event is identified as an electron with a tight Gas Cerenkov cut.
- (4) The event is in a good acceptance region of the spectrometer.
- (5) The event is in the central region of the block being calibrated.

### 3.2 The method for determination of NaI (Tl) calibration coefficients

The calibration coefficients are defined to transform the ADC amplitude of each block into the energy deposition of the electron in this block. Since the Moliere radius of NaI (Tl) is 4.8 cm [5], the incident particle's energy is deposited in the 9 blocks when it hits the central block (i.e. blk5 in Fig. 1). The basic calibration cell is set to be 9 blocks. A linear minimization method is used to determine the calibration coefficients. The Chi-square minimization function is defined as follows,

$$\chi^2 = \sum_{j=0}^N \left( E_{\text{kin}}^j - \sum_{k=0}^9 C_k A_k^j \right)^2, \quad (2)$$

where  $j$  is the index of the selected calibration events and  $k$  is the index of the NaI (Tl) blocks.  $A_k^j$  is the amplitude in the  $k$ -th NaI (Tl) block for the  $j$ -th event.  $E_{\text{kin}}$  is the scattering electron energy;  $C_k$  is

the calibration constant for the  $k$ -th block,

$$\frac{\partial}{\partial C_i} \chi^2 = \frac{\partial}{\partial C_i} \sum_{j=0}^N \left( E_{\text{kin}}^j - \sum_{k=0}^9 C_k A_k^j \right)^2, \quad (3)$$

where  $i$  varies between 0 and 9.  $\chi^2$  is minimized when the above quantity is set to zero. It leads to

$$\sum_{k=0}^9 \left( C_k \left( \sum_{j=0}^N A_k^j A_j^j \right) \right) = \sum_{j=0}^N E_{\text{kin}}^j A_i^j. \quad (4)$$

The linear equation can be summarized in matrix form ...

$$MC = E, \quad (5)$$

where  $C$  and  $E$  are defined as vectors

$$C = \begin{pmatrix} C_0 \\ \cdot \\ \cdot \\ \cdot \\ C_n \end{pmatrix}, \quad (6)$$

$$E = \begin{pmatrix} \sum_{j=0}^N E_{\text{kin}}^j A_0^j \\ \cdot \\ \cdot \\ \cdot \\ \sum_{j=0}^N E_{\text{kin}}^j A_n^j \end{pmatrix}, \quad (7)$$

and the matrix elements are given by

$$M_{ij} = \sum_{k=0}^N A_i^k A_j^k. \quad (8)$$

At the end, the calibration coefficients are obtained by inverting as (5)

$$C = M^{-1} E. \quad (9)$$

### 3.3 Missing energy correction for bad blocks

To find an average value to correct for the missed energy in the neighboring block that is bad, 9 good blocks are selected for studying the amplitude ratio of adjacent block to the central one. After obtaining the relationship, the missing energy of bad blocks could be corrected back for calibration. A few small circle cuts in the region of the central block are set to obtain the amplitude ratio for scattering electrons with  $p=539$  MeV/ $c$  at  $60^\circ$ .

The amplitude ratios of adjacent blocks to the central one ( $|x| < 0.03$  m,  $|y| < 0.03$  m) are fitted to 2nd-order polynomials in two dimensions. The fol-

lowing relations are obtained,

$$R1 = 0.01473 - 0.09517x + 7.359x^2 + 0.1848y + 7.51y^2, \quad (10)$$

$$R2 = 0.01402 - 0.3942x + 8.537x^2 - 0.001413y - 2.994y^2, \quad (11)$$

$$R3 = 0.01399 - 0.1175x + 4.114x^2 - 0.1725y + 4.55y^2, \quad (12)$$

$$R4 = 0.02414 - 0.08904x + 21.29x^2 + 0.8816y + 23.54y^2, \quad (13)$$

$$R5 = 1, \quad (14)$$

$$R6 = 0.02423 - 0.001044x + 19.357x^2 - 0.5776y + 9.302y^2, \quad (15)$$

$$R7 = 0.008895 - 0.09234x + 6.1917x^2 + 0.09544y + 4.266y^2, \quad (16)$$

$$R8 = 0.01739 + 0.7615x + 22.78x^2 + 0.01578y + 5.965y^2, \quad (17)$$

$$R9 = 0.01359 + 0.1170x + 7.258x^2 - 0.2098y + 7.97y^2, \quad (18)$$

where  $R1$ ,  $R2$ ,  $R3$ ,  $R4$ ,  $R5$ ,  $R6$ ,  $R7$ ,  $R8$  and  $R9$  are the amplitude ratios of each adjacent block to the central block, respectively.  $x$  and  $y$  represent the vertical and horizontal directions shown in Fig. 1 Since the amplitude ratios of adjacent blocks have a momentum dependence, different math forms are taken for different momentum settings for which calibrations are performed.

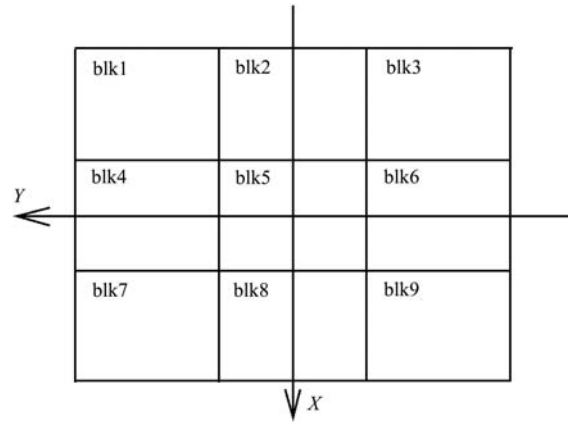


Fig. 1. 9 blocks scheme for NaI (TI) calibration.

## 4 Checking the calibration results

The energy deposition  $E$  of an incident electron

in the calorimeter detector could be calculated with the calibration constants  $C$  by the following formula,

$$E = \sum_{i=0}^{90} C_i \cdot A_i, \quad (19)$$

where  $i$  is the number of NaI (Tl) detector block. The  $E/p$  of electrons should be around 1 after the calibration correction where  $E$  is the total deposit energy calculated from Eq. (19) and  $p$  is the momentum. The  $E/p$  plot before calibration is shown in Fig. 2 at 120 MeV of scattering electron. The plot after calibration correction is shown in Fig. 3.

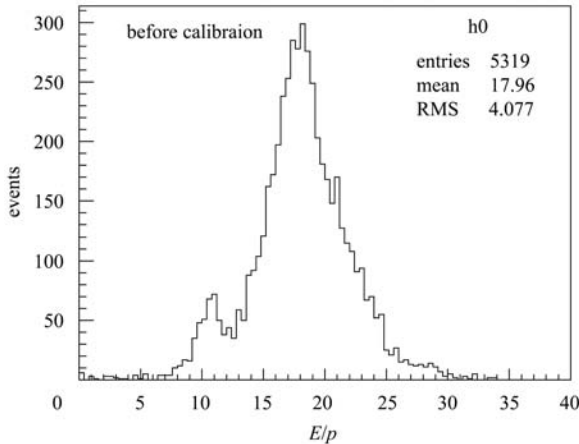


Fig. 2. The  $E/p$  plot before calibration for a non-calibration run.

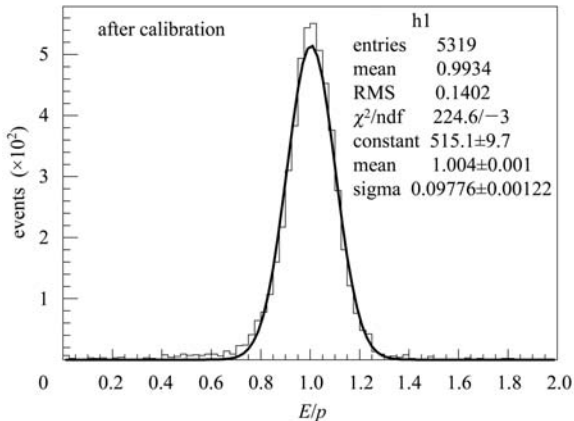


Fig. 3.  $E/p$  plot after calibration for the electron peak of a non-calibration run.

The  $E/p$  plot for electrons should be a Gaussian distribution plus a tail. The width of the Gaussian distribution represents the detector's resolution. Fig. 3 shows a reasonable spectrum after calibration correction.

The events at the low momentum tail are electrons with energy leakage, electrons that scattered the walls of the spectrometer and secondary productions, including electrons and hadrons. The energy resolution

of  $E/p$  in Fig. 3 is about 9.7% for 120 MeV at this HV setting and the best resolution we can reach is 3% for 1 GeV. Due to a large set of kinematics and the changes in HV for the NaI (Tl) detector during the data-taking period, different sets of calibration constants are needed for this experiment. A total of 40 sets of constants for production runs are obtained for this experiment.

## 5 NaI (Tl) simulation for background analysis

A simulation using SNAKE [6] and GEANT3 [7] was performed when the experiment was proposed [2]. We used that to generate an input electron sample for the NaI (Tl) detector. GEANT4 is used for NaI (Tl) detector simulation.

### 5.1 SNAKE and GEANT3 simulation

The background generated by the interaction of electrons with the inner walls of the spectrometer magnets is studied with a Monte-Carlo simulation. The simulation is based on a ray-tracing program, SNAKE. In the original version of SNAKE, an electron hitting the internal boundaries of the spectrometer is considered lost. In the modified version of the simulation program, the electron is studied further with a GEANT3 simulation for one of two possibilities: (a) scattering off the wall; (b) generation of secondary particles from an interaction with the wall material.

Then the rescattered electron or the secondary particles are re-inserted into the SNAKE simulation and are traced to the focal plane. Since particles hitting the walls of Q1, Q2 could not make it to the focal plane and the ones hitting the dipole have low probabilities of reaching the focal plane in the SNAKE simulations. So the simulation is focused on the interaction of electrons with the walls of the Q3 magnet. Due to the proximity of the Q3 magnet to the focal plane, electrons bouncing off the surface of the Q3 magnet would have a higher probability of survival than those bouncing off the other magnets. The result of simulation shows that the background generated in this process is about 1.2% of the clean events at a spectrometer momentum setting of 120 MeV/c, the lowest momentum setting among our kinematics. A few background events with energy comparable to clean events came from a single, large angle scattering on the surface of the Q3 magnet. With a tight cut on the position on the focal plane, about 80%

of the background events are eliminated. This is in agreement with the results from an independent analysis [8]. The remaining background events after the focal plane position cut can be eliminated by an independent energy measurement such as the NaI (Tl) calorimeter. The position and momentum direction

of the electron sample before entering the NaI (Tl) detector, which are generated from the SNAKE and GEANT3 simulation, are shown in Fig. 4 (a) and (b), respectively. The electrons reflected by the Dipole and Q3 contributed about 0.24%, 1.2% background, respectively.

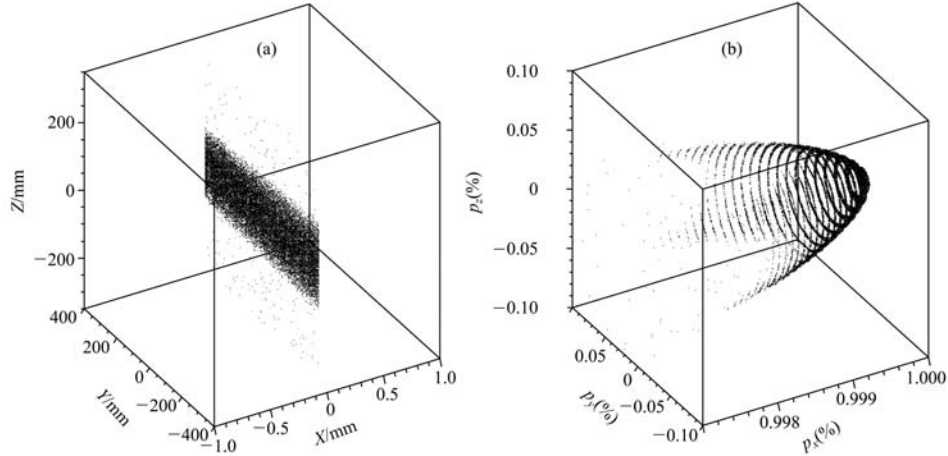


Fig. 4. The position and direction of the electron sample generated by SNAKE and GEANT3 at a momentum setting of 120 MeV.

Figure 5 shows the energy distribution for the electron sample. The good electron peak (dashed line) is at 120 MeV and the background (solid line) spreads out, which are electrons scattered by Dipole and Q3 magnets. The electrons are re-inserted into GEANT4 to simulate their behavior in the NaI (Tl) detector.

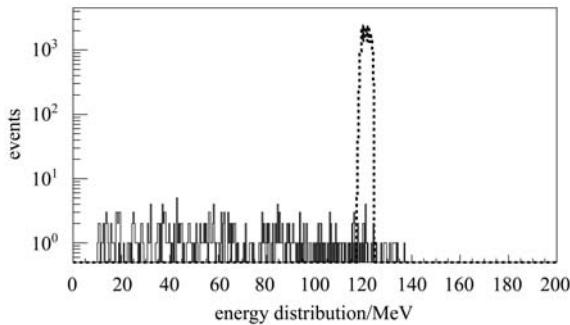


Fig. 5. The energy distribution of the electron sample generated by SNAKE and GEANT3 at a momentum setting of 120 MeV.

## 5.2 NaI (Tl) GEANT4 simulation

The geometry of the NaI (Tl) detector is shown in Fig. 6. The parameters used in the GEANT4 simulation for NaI (Tl) properties are obtained from the manufacture [9]. The trajectories of electrons and photons are shown in Fig. 6. Since the input electron

energy is 120 MeV, the total energy of the electron is absorbed by the NaI (Tl) calorimeter.

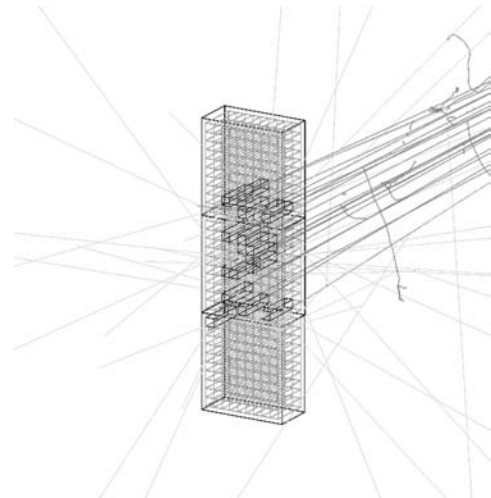


Fig. 6. Visualization of GEANT4 simulation for the NaI (Tl) detector at a momentum setting of 120 MeV of scattering electrons (line from right to left).

## 5.3 A comparison between data and simulation for 120 MeV and 539 MeV

Figure 7 shows, in log scale, the distribution of energy deposition by electrons in the NaI (Tl) detector for the simulation result (dashed line) and data

(solid line), respectively. Since the simulation did not contain intrinsic resolution of spectrometers (Dipole, Quadrupoles), the simulation only reproduces the low energy part of the Gaussian distribution after electron deposited energy in the NaI (Tl) middle box. Because the background of rescattered electrons inside spectrometers is the main issue for low-energy/backward-angle data, it can be ignored for high-energy/forward-angle data due to good optics. As this kind of background distributes mainly at low energy side, in our case the asymmetry of the simulation result has no effect on the background analysis.

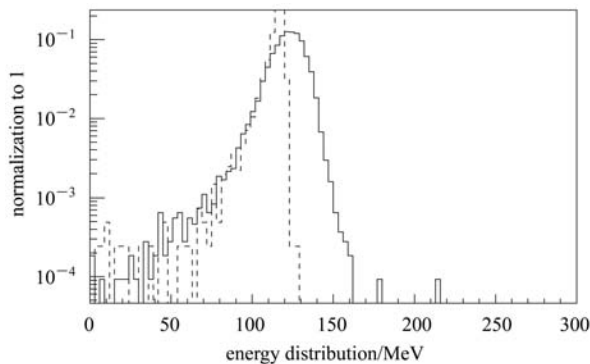


Fig. 7. Comparison between data (solid line) and simulation (dashed line) at a momentum setting of 120 MeV with log scale.

The good match between simulation and real data in the low energy part of the distribution is shown in Fig. 7 for 120 MeV of scattering electrons. From the simulation result, the contamination from scattering off walls of the Dipole and Q3 is about 0.31% and the electron selection efficiency is 99.9% after adding a cut on the energy distribution at 50 MeV for this kinematic setting.

Figure 8 shows a comparison between the simulation and data for scattering electrons with momenta of 539 MeV. With a cut applied at 150 MeV, the residual contamination from surface scattering from

the Dipole and Q3 is about 0.029% and the electron selection efficiency is 99.9%.

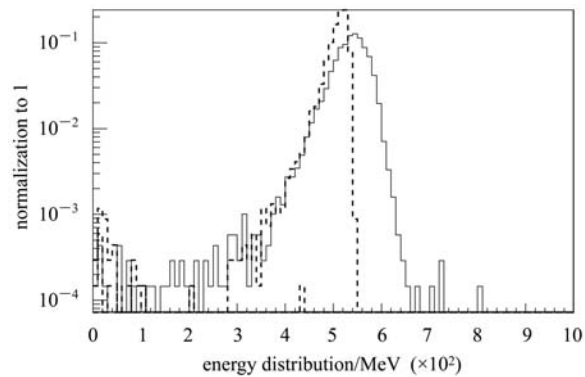


Fig. 8. Comparison between the data (solid line) and simulation (dashed line) for 539 MeV with a log scale.

## 6 Conclusion

The NaI (Tl) detector has been well calibrated for the Coulomb sum rule experiment. Corrections are applied to the missing energy due to a few inefficient detector blocks. Because of the large set of kinematics and the changes in HVs, 40 sets of calibration constants are obtained. The energy resolution of the NaI (Tl) detector reached  $\frac{\delta E}{\sqrt{E}} \approx 3\%$  for 1 GeV electrons. We also carried out a simulation to study the background due to re-scattering from the inner walls of the Dipole and Q3 for the spectrometer momentum settings of 120 MeV and 539 MeV. The contamination is about 0.3% and 0.03% when cuts at 50 MeV and 150 MeV are applied for the momentum settings of 120 MeV and 539 MeV, respectively (see Fig. 7 and Fig. 8). With the same cuts, the electron selection efficiency is 99.9% for both settings. The good calibration and background analysis of the NaI (Tl) detector is very helpful for the reduction of systematic error of cross section and the separation of  $R_L$  and  $R_T$ .

## References

- 1 Morgenstern J, Meziani Z E. Phys. Lett. B, 2001, **515**: 269–275
- 2 CHEN J P, Choi S, Meziani Z E (Spokespersons). Jefferson Lab E05-110
- 3 Alcorn J et al. Nuclear Instruments and Methods in Physics Research A, 2004, **522**: 294–346
- 4 WILSON S L et al. Nuclear Instruments and Methods in Physics Research A, 1988, **264**: 263–284
- 5 ZHU R Y. Nuclear Instruments and Methods in Physics Research A, 1998, **413**: 297–311
- 6 <http://hallaweb.jlab.org/news/minutes/tranferfuncs.html>
- 7 <http://www.pv.infn.it/sc/cern/geant.pdf>
- 8 Arrington J. Presentation given at JLab E01-001 collaboration meeting, 2003
- 9 [http://www.detectors.saint-gobain.com/NaI\(Tl\).aspx](http://www.detectors.saint-gobain.com/NaI(Tl).aspx)